Entropy Effects in the Fragmentation of 1,1-Dimethylhydrazine Ions

Anne-Marie Boulanger,[†] Emma E. Rennie,[†] David M. P. Holland,[‡] David A. Shaw,[‡] and Paul M. Mayer*,[†]

Chemistry Department, University of Ottawa, Ottawa, Ontario K1N 6N5, Canada, and Daresbury Laboratory, Daresbury, Warrington, Cheshire WA4 4AD, United Kingdom

Received: November 27, 2006; In Final Form: March 13, 2007

The 1,1-dimethylhydrazine ion (($CH_3)_2NNH_2^{+\bullet}$) has two low-energy dissociation channels, the loss of a hydrogen atom to form the fragment ion m/z 59, $(CH_3)(CH_2)NNH_2^+$, and the loss of a methyl radical to form the fragment ion m/z 45, the methylhydrazyl cation, $CH_3NNH_2^+$. The dissociation of the 1,1-dimethylhydrazine ion has been investigated using threshold photoelectron−photoion coincidence (TPEPICO) spectroscopy, in the photon energy range 8.25−31 eV, and tandem mass spectrometry. Theoretical breakdown curves have been obtained from a variational transition state theory (VTST) modeling of the two reaction channels and compared to those obtained from experiment. Seven transition states have been found at the B3-LYP/6-31+G(d) level of theory for the methyl radical loss channel in the internal energy range of 2.32−3.56 eV. The methyl loss channel transition states are found at R_{N-C} = 4.265, 4.065, 3.965, 3.165, 2.765, 2.665, and 2.565 Å over this internal energy range. Three transition states have been found for the hydrogen atom loss channel: R_{H-C} = 2.298, 2.198, and 2.098 Å. The $\Delta S^\ddagger(45)$ value, at an internal energy of 2.32 eV and a bond distance of R_{N-C} = 4.265 Å, is 65 J K^{-1} mol^{-1}. As the internal energy increases to 3.56 eV the variational transition state moves to lower R value so that at R_{N-C} = 2.565 Å, the $\Delta S^\ddagger$ decreases to 29 J K^{-1} mol^{-1}. For the hydrogen atom loss channel the variation in $\Delta S^\ddagger$ is less than that for the methyl loss channel. To obtain agreement with the experimental breakdown curves, $\Delta S^\ddagger(59)$ = 26−16 J K^{-1} mol^{-1} over the studied internal energy range. The 0 K enthalpies of formation ($\Delta_f H_0$) for the two fragment ions m/z 45 and m/z 59 have been calculated from the 0 K activation energies (E_0) obtained from the fitting procedure: $\Delta_f H_0[CH_3NNH_2^+]$ = 906 ± 6 kJ mol^{-1} and $\Delta_f H_0[(CH_3)(CH_2)NNH_2^+]$ = 822 ± 7 kJ mol^{-1}. The calculated G3 values are $\Delta_f H_0[CH_3NNH_2^+]$ = 911 kJ mol^{-1} and $\Delta_f H_0[(CH_3)(CH_2)NNH_2^+]$ = 825 kJ mol^{-1}. In addition to the two low-energy dissociation products, 21 other fragment ions have been observed in the dissociation of the 1,1-dimethylhydrazine ion as the photon energy was increased. Their appearance energies are reported.

Introduction

A unimolecular reaction is defined as any system evolving in time as a result of excitation.[1] An activated unimolecular reaction[2] consists of two steps: first the activation−deactivation step (1) and second the unimolecular dissociation (2):

$$AB + M \text{ (or } h\nu) \leftrightarrow AB^* + M \text{ (or } h\nu) \qquad (1)$$

$$AB^* \rightarrow A + B \qquad (2)$$
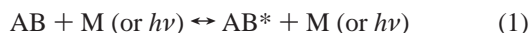
This type of reaction follows an exponential decay and assumes that the dissociation rate is dependent on the internal energy of the molecule.

Transition state theory (TST) can be used to determine the entropy of activation, $\Delta S^\ddagger$, of unimolecular reactions. In the thermodynamic version of TST, the Arrhenius pre-exponential factor A can be written in terms of $\Delta S^\ddagger$:

$$A = \frac{k_B T}{h} e^1 e^{\Delta S^\ddagger/R} \qquad (3)$$

where k_B is Boltzmann's constant, T is temperature, h is Planck's constant, and R is the gas constant.
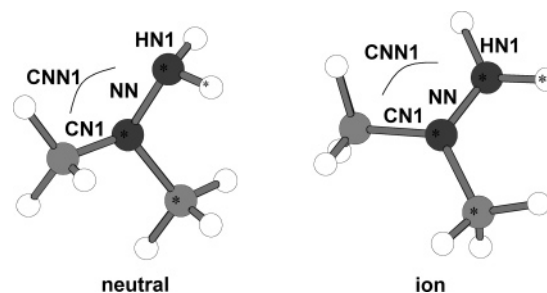

Figure 1. Neutral and ionized 1,1-dimethylhydrazine optimized structures. The nitrogen atoms are dark gray, the carbon atoms are light gray, and the hydrogen atoms are white. The asterisks (*) show the four atoms involved in the HNNC dihedral angle (see Table 1 for values).

Experimentally, the $\Delta S^\ddagger$ for a bond cleavage in a gas-phase ion can be determined directly from the temperature dependence[3] of the unimolecular reaction using an Arrhenius plot. However, it can be difficult to perform such experiments in a mass spectrometer because of the low pressures used in the instrument and the large binding energies typical of gas-phase ions. Often the potential energy curve for the reaction $A^+ \rightarrow B^+ + C$ has a maximum (saddle-point) between A^+ and products corresponding to the transition state of the reaction and thus the 0 K activation energy E_0, and the $\Delta S^\ddagger$ can be determined from ab initio calculations. However, in most bond cleavage reactions,

* Corresponding author. E-mail: pmmayer@uottawa.ca.
† University of Ottawa.
‡ Daresbury Laboratory.

Fragmentation of 1,1-Dimethylhydrazine Ions

J. Phys. Chem. A, Vol. 111, No. 25, 2007 **5389**

TABLE 1: Optimized Geometric Parameters of Neutral and Ionized 1,1-Dimethylhydrazine

basis set	R_{NN}	R_{CN1}	R_{CN2}	R_{HN1}	R_{HN2}	∠CNN1	∠CNN2	∠HNNC[a]
Neutral 1,1-Dimethylhydrazine								
HF								
6-31G(d)	1.408	1.445	1.445	1.001	1.008	109.3	113.0	−40.2
6-31+G(d)	1.408	1.446	1.447	1.000	1.008	109.3	112.9	−40.3
6-311G(d)	1.406	1.445	1.445	0.997	1.005	109.4	112.9	−40.0
6-311G(d,p)	1.406	1.446	1.446	0.999	1.007	109.4	112.9	−40.8
6-311+G(d,p)	1.406	1.446	1.447	0.999	1.006	109.5	112.9	−40.7
6-311G(df,p)	1.404	1.443	1.444	0.998	1.006	109.6	113.0	−41.4
6-311G(2df,p)	1.405	1.442	1.443	0.999	1.006	109.5	112.9	−41.5
6-311+G(2df,p)	1.404	1.443	1.443	0.998	1.006	109.6	112.9	−41.5
MP2								
6-31G(d)	1.433	1.456	1.457	1.020	1.030	107.3	111.7	−40.2
6-31+G(d)	1.432	1.458	1.460	1.019	1.030	107.7	112.1	−39.5
6-311G(d)	1.426	1.454	1.456	1.013	1.023	107.6	111.7	−39.1
6-311G(d,p)	1.427	1.455	1.457	1.016	1.027	107.4	111.5	−41.0
6-311+G(d,p)	1.426	1.456	1.458	1.016	1.026	107.8	111.8	−40.0
6-311G(df,p)	1.420	1.448	1.451	1.014	1.025	107.7	111.8	−41.3
6-311G(2df,p)	1.427	1.450	1.452	1.016	1.027	107.3	111.5	−41.2
6-311+G(2df,p)	1.426	1.451	1.453	1.016	1.026	107.6	111.7	−40.6
B3-LYP								
6-31G(d)	1.430	1.456	1.457	1.019	1.031	108.4	112.6	−41.4
6-31+G(d)	1.429	1.458	1.460	1.018	1.029	108.7	112.8	−41.1
6-311G(d,p)	1.428	1.456	1.458	1.015	1.027	108.7	112.7	−41.7
6-311+G(d,p)	1.427	1.457	1.459	1.015	1.026	109.0	112.8	−41.1
Ionized 1,1-Dimethylhydrazine								
HF								
6-31G(d)	1.312	1.465	1.465	1.000	1.000	117.9	117.9	−28.0
6-31+G(d)	1.313	1.465	1.465	1.000	1.000	117.9	117.9	−27.9
6-311G(d)	1.311	1.464	1.464	0.996	0.996	117.9	117.9	−28.5
6-311G(d,p)	1.310	1.465	1.465	0.998	0.999	118.0	118.0	−27.0
6-311+G(d,p)	1.311	1.465	1.465	0.999	0.999	118.0	118.0	−27.2
MP2								
6-31G(d)	1.324	1.462	1.462	1.018	1.018	117.0	117.0	−28.7
6-31+G(d)	1.325	1.463	1.463	1.019	1.019	116.8	116.8	−29.5
6-311G(d)	1.319	1.461	1.461	1.013	1.013	117.1	117.1	−29.0
6-311G(d,p)	1.319	1.462	1.462	1.015	1.015	117.2	117.2	−29.0
6-311+G(d,p)	1.320	1.462	1.462	1.015	1.015	117.1	117.1	−29.3
6-311G(df,p)	1.315	1.455	1.455	1.014	1.014	117.3	117.0	−27.5
B3-LYP								
6-31G(d)	1.333	1.464	1.464	1.017	1.017	117.6	117.6	−28.9
6-31+G(d)	1.334	1.465	1.465	1.017	1.017	117.6	117.6	−28.7
6-311G(d,p)	1.330	1.463	1.463	1.014	1.014	117.8	117.8	−26.6
6-311+G(d,p)	1.330	1.463	1.463	1.014	1.014	117.8	117.8	−26.4

[a] The atoms involved in the HNNC dihedral angle are identified by an asterisk (*) in Figure 1.

the potential energy curve does not have a maximum between the reactants and the products, and the location of the transition state is not properly defined.[4] Therefore, the calculation of the $\Delta S^{\ddagger}$ is difficult. Variational transition state theory (VTST) can be used to treat unimolecular dissociations to identify the transition state and thus calculate $\Delta S^{\ddagger}$ values. VTST allows one to choose the transition state to be the dividing surface between the reactants and the products that corresponds to the smallest rate constant.[4] This corresponds to a local minimum in the sum-of-states and is called an "entropy" bottleneck. The rate constant can be related to the transition state sum-of-states by the following RRKM/QET expression:[1]

$$k(E_{int}) = \frac{\sigma}{h} \frac{N^{\ddagger}(E_{int}, E_0, R^*)}{\rho(E_{int})} \qquad (4)$$

where $k(E_{int})$ is the unimolecular rate constant at an ion internal energy E_{int}, σ is the reaction symmetry number, h is Planck's constant, $\rho(E_{int})$ is the reactant ion density of states, and $N^{\ddagger}(E_{int}, E_0, R^*)$ is the sum-of-states for the dissociation bottleneck located at a bond distance R^*.

The goal of this study was to examine the impact that $\Delta S^{\ddagger}$ can have on an otherwise simple unimolecular dissociation

reaction: a bond cleavage. 1,1-Dimethylhydrazine ions were chosen because, as will be evident from the experimental data obtained for this ion, the reactions leading to the loss of an H atom and a methyl group exhibit significant entropy effects. Our approach was to model the ion decomposition as a function of internal energy and compare the results with those from threshold photoelectron−photoion coincidence (TPEPICO) spectroscopy. It was necessary in this process to employ a simple VTST treatment to learn about the $\Delta S^{\ddagger}$ for the two competing dissociation channels of this ion. The entropy of activation has a significant impact on the dissociation of the parent ion, and this is described in detail. The large change in $\Delta S^{\ddagger}$ as the internal energy increases affects the shape of the breakdown curves and their variational fits. The modeling further permits the determination of reliable enthalpies of formation for the two fragment ions in question. In addition, appearance energies (AEs) for higher energy fragmentation pathways have been measured for photon energies up to 31 eV.

Experimental Procedures

Experimental Overview. The TPEPICO experiments have been carried out at the Daresbury Laboratory synchrotron radiation source. The TPEPICO spectrometer,[5] the 5 m normal

TABLE 2: Comparison of the Absolute and Relative Energies[a] of the Fragment Ions and Neutrals of the 1,1-Dimethylhydrazine Ion at Four Different Levels of Theory (HF, MP2, B3-LYP, and G3)[b]

basis set	$(CH_3)_2NNH_2^{+•}$		$(CH_3)(CH_2)NNH_2^+ + H^•$		$(CH_3)_2NNH^+ + H^•$		$CH_3NNH_2^+ + CH_3^•$	
	absolute	relative	absolute	relative	absolute	relative	absolute	relative
HF								
6-31G(d)	−188.902152	0	−188.824145	205	−188.811742	237	−188.825910	200
6-31+G(d)	−188.904294	0	−188.826756	204	−188.813387	239	−188.829297	197
6-311G(d)	−188.941709	0	−188.865275	201	−188.851718	236	−188.867304	195
6-311G(d,p)	−188.958312	0	−188.880293	205	−188.865533	244	−188.884236	194
6-311+G(d,p)	−188.959983	0	−188.881935	205	−188.866928	244	−188.886041	194
MP2								
6-31G(d)	−189.465208	0	−189.395065	184	−189.389121	200	−189.375940	234
6-31+G(d)	−189.472776	0	−189.402854	184	−189.395293	203	−189.384105	233
6-311G(d)	−189.535327	0	−189.465026	185	−189.458419	202	−189.448138	229
6-311G(d,p)	−189.594696	0	−189.518016	201	−189.510232	222	−189.506884	231
6-311+G(d,p)	−189.599093	0	−189.522453	201	−189.514200	223	−189.510844	232
B3-LYP								
6-31G(d)	−190.120277	0	−190.030283	236	−190.018794	266	−190.028875	240
6-31+G(d)	−190.123694	0	−190.034085	235	−190.021522	268	−190.035425	232
6-311G(d,p)	−190.177649	0	−190.089055	233	−190.074061	272	−190.084414	245
6-311+G(d,p)	−190.179472	0	−190.091025	232	−190.075634	273	−190.092264	229
G3[c]	−190.034442	0	−189.954131	211	−189.940264	247	−189.946822	230

[a] Absolute energies are in hartrees and relative energies are in kJ mol^{-1}; the energies have been corrected for ZPE. [b] The 1,1-dimethylhydrazine ion, $(CH_3)(CH_2)NNH_2^+$, and $(CH_3)_2NNH^+$ belong to the C_1 point group, $CH_3NNH_2^+$ belongs to the C_s point group, and the methyl radical belongs to the D_{3h} point group. [c] A modified G3[11,12] protocol based on optimized B3-LYP/6-31+G(d) geometries and scaled B3-LYP ZPE.

incidence monochromator,[6] and the experimental procedures[7,8] have been described in detail previously.

A pulsed extraction technique allowed the breakdown curve to be recorded as a function of parent ion residence time in the interaction region by changing the time between the detection of the threshold electron and the application of the ion drawout field.[5,8] The residence time is defined as the period between the creation of the electron-ion pair and the application of the pulse and is given by the transit time of the electron added to the electronic signal processing time. The minimum residence time in the current apparatus has been measured as 1.116 ± 0.050 μs using the experimental procedure described in Holland et al.[5] The breakdown curve of 1,1-dimethylhydrazine in the first cross-over region (between $h\nu \approx 9.4$ and 10.4 eV) has been measured for four ion residence times: 1.116, 3.116, 5.116, and 7.116 μs. The electron transmission function used in the convolution of the calculated breakdown curves was derived from a threshold electron spectrum obtained from the photoionization of krypton in the region of the $^2P_{1/2}$ ionization limit under the conditions used in the TPEPICO measurements.[5]

The mass-analyzed ion kinetic energy (MIKE) and collision-induced dissociation (CID) experiments were performed on a modified VG ZAB mass spectrometer[9] incorporating a magnetic sector followed by two electrostatic sectors (BEE geometry). Ions were generated in the ion source by electron ionization. The pressure inside the ion source was kept at ~1.0×10^{-5} Torr as measured with an ionization gauge located above the ion source diffusion pump. CID experiments were performed using helium as the target gas. The helium pressure in the collision cell was approximately 8.0×10^{-8} Torr to 1.0×10^{-7} Torr corresponding to a beam reduction of 10%. Deuterium exchange experiments were done with D_2O. The glass capillary inlet was flushed four times with 10 μL of deuterium oxide prior to the introduction of 1,1-dimethylhydrazine. A peak with m/z 62 was observed corresponding to the deuterated 1,1-dimethylhydrazine ion ($(CH_3)_2NND_2^{+•}$).

Materials. 1,1-Dimethylhydrazine (Lancaster, 98%) and deuterium oxide (MSD Isotopes, 99.9% D) were used without further purification for the MIKE and CID experiments.

The TPEPICO experiments were performed with 1,1-di-methylhydrazine (>97%) obtained from Aldrich. The sample was subjected to three freeze−pump−thaw cycles to remove air.

Computational Procedures. Ab initio molecular orbital calculations were performed using the Gaussian 98[10] suite of programs. The 1,1-dimethylhydrazine ion and all fragment ions and neutrals were optimized at the B3-LYP/6-31+G(d) level of theory. This basis set was chosen because it adequately described the geometry and vibrational frequencies of the 1,1-dimethylhydrazine ion when compared to larger basis sets. The optimized geometric parameters of neutral and ionic 1,1-dimethylhydrazine are listed in Table 1 and shown in Figure 1. The neutral molecule has been optimized at three different levels of theory with eight different basis sets, from 6-31G(d) up to 6-311+G(2df,p), except at the B3-LYP level of theory where four basis sets were used. Ionized 1,1-dimethylhydrazine was optimized at the same three levels of theory with basis sets ranging from 6-31G(d) up to 6-311+G(d,p). Similar geometrical parameters were obtained at the MP2 and B3-LYP levels of theory. The HF bond lengths were always shorter than those calculated using the MP2 or B3-LYP methods. As the basis set size was increased from 6-31G(d) to 6-311+G(2df,p), we observed that the geometries of both neutral and ionic 1,1-dimethylhydrazine did not vary significantly. From these observations, we concluded that it was not necessary to use a large basis set, such as 6-311+G(2df,p), to perform our calculations because the results were similar to those obtained using 6-31+G(d). The MP2 treatment was discarded in this theoretical study because it gave results for the dissociation energies that were contrary to the experimental results. The two possible dissociation channels resulting in hydrogen atom loss, either $[(CH_3)(CH_2)NNH_2^+ + H^•]$ or $[(CH_3)_2NNH^+ + H^•]$, were much lower in energy at the MP2 level of theory than the methyl loss channel, $[CH_3NNH_2^+ + CH_3^•]$. In the B3-LYP treatment, the relative energies of the fragments were more consistent with the MIKE and CID experimental results. Table 2 lists the absolute and relative energies of the 1,1-dimethylhydrazine ion and its dissociation products at the three different levels of theory mentioned previously with the five different basis sets. A

Fragmentation of 1,1-Dimethylhydrazine Ions

J. Phys. Chem. A, Vol. 111, No. 25, 2007 **5391**

TABLE 3: Transition States, Entropies of Activation (600 K) and Activation Energies (0 K) for the Unimolecular Dissociations of the 1,1-Dimethylhydrazine Ion at the B3-LYP/6-31+G(d) Level of Theory in the Internal Energy Range of 2.32−3.56 eV

dissociation channel	$CH_3NNH_2^+ + CH_3^\bullet$							
B3-LYP/6-31+G(d)	$\Delta E^a = 2.295$ eV or 221.5 kJ mol^{-1}							
R^* (Å)	2.565	2.665	2.765	3.165	3.965	4.065	4.265	
$\Delta S^\ddagger$ (J K^{-1} mol^{-1})	28.9	31.5	34.2	43.1	59.4	60.5	65.4	
E_0 (eV)	2.105	2.138	2.162	2.226	2.285	2.289	2.293	
corrected to G3 product energy	$\Delta E = 2.391$ eV or 230.6 kJ mol^{-1}							
R^* (Å)	2.565	2.665	2.765	3.165	3.965	4.065	4.365	
$\Delta S^\ddagger$ (J K^{-1} mol^{-1})	28.9	31.5	34.2	43.1	59.4	60.5	67.0	
E_0 (eV)	2.200	2.233	2.257	2.322	2.381	2.384	2.390	
fit 1	$\Delta E = 2.325$ eV or 224.4 kJ mol^{-1}							
R^* (Å)	2.565	2.665	2.765	3.165	3.965	4.065	4.265	
$\Delta S^\ddagger$ (J K^{-1} mol^{-1})	28.9	31.5	34.2	43.1	59.4	60.5	65.4	
E_0 (eV)	2.135	2.168	2.192	2.256	2.315	2.319	2.323	
fit 2	$\Delta E = 2.330$ eV or 224.8 kJ mol^{-1}							
R^* (Å)	2.565	2.665	2.765	2.865	3.165	3.965	4.065	4.265
$\Delta S^\ddagger$ (J K^{-1} mol^{-1})	28.9	31.5	34.2	36.4	43.1	59.4	60.5	65.4
E_0 (eV)	2.140	2.173	2.197	2.217	2.261	2.320	2.324	2.328
fitting with one transition state	$\Delta E = 2.355$ eV or 227.2 kJ mol^{-1}							
R^* (Å)	3.46							
$\Delta S^\ddagger$ (J K^{-1} mol^{-1})	43.3							
E_0 (eV)	2.314							

dissociation channel	$(CH_3)(CH_2)NNH_2^+ + H^\bullet$		
B3-LYP/6-31+G(d)	$\Delta E = 2.405$ eV or 232.1 kJ mol^{-1}		
R^* (Å)	2.098	2.198	2.298
$\Delta S^\ddagger$ (J K^{-1} mol^{-1})	0.9	4.5	7.9
E_0 (eV)	2.385	2.402	2.407
corrected to G3 product energy	$\Delta E = 2.185$ eV or 210.9 kJ mol^{-1}		
R^* (Å)	2.098	2.198	
$\Delta S^\ddagger$ (J K^{-1} mol^{-1})	0.9	4.5	
E_0 (eV)	2.165	2.182	
fit 1	$\Delta E = 2.180$ eV or 210.4 kJ mol^{-1}		
R^* (Å)	2.098	2.198	
$\Delta S^\ddagger$ (J K^{-1} mol^{-1})	21.9	25.6	
E_0 (eV)	2.160	2.177	
fit 2	$\Delta E = 2.155$ eV or 208.0 kJ mol^{-1}		
R^* (Å)	2.098	2.198	
$\Delta S^\ddagger$ (J K^{-1} mol^{-1})	18.9	22.6	
E_0 (eV)	2.135	2.152	
fit 3	$\Delta E = 2.130$ eV or 205.6 kJ mol^{-1}		
R^* (Å)	2.098	2.198	
$\Delta S^\ddagger$ (J K^{-1} mol^{-1})	16.2	19.9	
E_0 (eV)	2.110	2.127	
fitting with one transition state	$\Delta E = 2.155$ eV or 208.0 kJ mol^{-1}		
R^* (Å)	2.20		
$\Delta S^\ddagger$ (J K^{-1} mol^{-1})	23.8		
E_0 (eV)	2.152		

^{a} Energy difference between the equilibrium ion and the plateau on the potential energy curve (energy value taken at $R_{N-C} = 4.56$ Å or $R_{H-C} = 2.50$ Å).

modified G3 protocol[11,12] based on the optimized B3-LYP/6-31+G(d) geometries and scaled B3-LYP ZPE (scaling factor = 0.9806) was used to calculate the enthalpies of formation of the 1,1-dimethylhydrazine ion and the fragment ions and neutrals. The G3 energies are found in Table 2.

Two potential energy curves were calculated at the B3-LYP/6-31+G(d) level of theory, one for each unimolecular dissociation. The first curve corresponds to the loss of a methyl group, and hence to the cleavage of one N−C bond. The second curve corresponds to the loss of a hydrogen atom from a methyl group. The potential energy curves were generated by optimizing the geometry of the dissociating ion by incrementally increasing the bond length by 0.1 Å until the energy reached a plateau at the separated products. This meant optimizing structures from the equilibrium bond length $R_{N-C} = 1.46$ Å to 6.21 Å for the

methyl loss channel and for hydrogen loss, between $R_{H-C} = 1.10$ Å and $R_{H-C} = 2.50$ Å. The vibrational frequencies and rotational constants were also calculated at each step. To assess the use of the 6-31+G(d) basis set, single-point energy calculations on the B3-LYP/6-31+G(d) geometries were performed with seven other basis sets ranging from 6-31G(d) to 6-311+G(2df,p). The relative energy (compared to the equilibrium structure) of a dissociating ion complex at a particular distance R_{X-C} did not change as the size of the basis set was increased, as shown in Figure S1 found in Supporting Information. Thus the B3-LYP/6-31+G(d) was a good level of theory to describe both unimolecular dissociations of the 1,1-dimethylhydrazine ions.

To calculate the rate constants ($k(E_{int})$) and the sum-of-states ($N^\ddagger$), a rovibrational RRKM approach was used. For each point
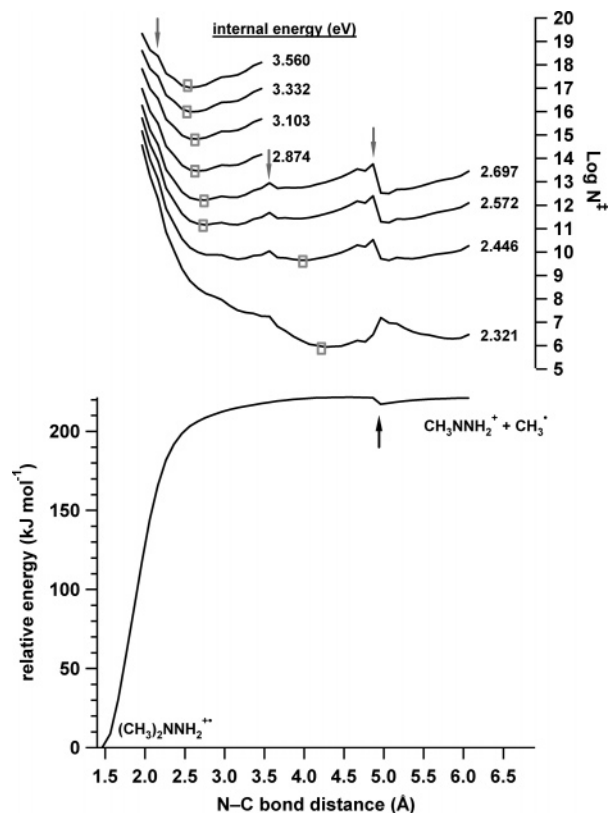
Figure 2. Potential energy curve for the loss of a methyl group from the 1,1-dimethylhydrazine ion and the sum-of-states as a function of the N−C bond distance calculated at the B3-LYP/6-31+G(d) level of theory. The gray arrows pointing down identify the local maxima in the sum-of-states. The squares correspond to the minima in $N^{\ddagger}$ and thus to the transition states for the N−C bond cleavage. The black arrow pointing up identifies the local minimum on the potential energy curve.

$R_{X−C}$, where X = N or H on the potential energy curve, the sum-of-states and rate constants were calculated. This was done by using the rotational constants and the scaled vibrational frequencies of the ion ($(CH_3)_2NNH_2^{+\bullet}$) as well as those of the dissociating complex at the bond distance $R_{X−C}$. An ion internal energy range (E_{min} = 2.32 eV and E_{max} = 3.56 eV) and a 0 K activation energy (E_0) were also defined (see Results and Discussion). A set of rate constants and sum-of-states as a function of internal energy (E_{int}) was generated by plotting the sum-of-states as a function of the bond distance $R_{X−C}$. At a given internal energy the minimum in the sum-of-states ($N^{\ddagger}_{min}$) corresponded to the transition state of the unimolecular dissociation.

To fit the experimental breakdown curves, the variational $k(E_{int})$ values for each channel were convoluted with the electron transmission function, the monochromator bandpass, and the thermal population distribution of the neutral 1,1-dimethylhydrazine molecule. The sets of rate constants were constructed by combining the rate constants corresponding to each transition state. For example, the set of rate constants for hydrogen loss ($k(59)$) at the B3-LYP/6-31+G(d) level of theory was constructed by taking the rate constants for TS(59)$_3$ from E_{int} = 2.424−2.526 eV, for TS(59)$_2$ from E_{int} = 2.527−2.991 eV, and for TS(59)$_1$ from E_{int} = 2.992−3.560 eV. Table S1 in Supporting Information contains an example of this VTST data. The transition states are listed in Tables 3 and S2 (Supporting Information).
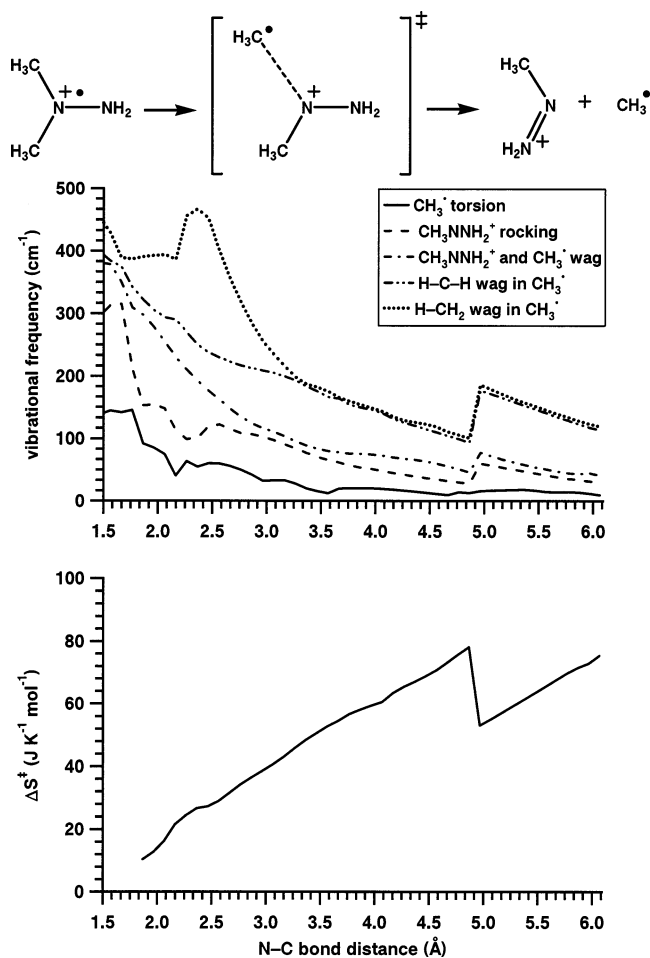

Figure 3. Five lowest vibrational frequencies of the methyl radical loss channel (top) and the entropy of activation (bottom) as a function of the N−C bond distance.

The neutral molecule population, $P(E_{int},T)$, was calculated up to an internal energy of 0.8 eV from eq 5:

$$P(E_{int},T) = \frac{P(E_{int})e^{-E_{int}/k_BT}}{Q(T)} \qquad (5)$$

where $P(E_{int})$ is the density of states and $Q(T)$ is the rovibrational partition function. The neutral molecule population was normalized such that the sum was equal to one.

Entropy Calculations. The statistical entropy (S) is calculated from the internal energy (E_{int}) of the molecule or ion and the partition functions (Q):[13]

$$S = \frac{E_{int}}{T} + Nk_B \ln Q \qquad (6)$$

We calculated the rovibrational entropy of activation, $\Delta S^{\ddagger}_{rovib}$, for both dissociation channels. To calculate the $\Delta S^{\ddagger}$ for methyl loss, the two methyl torsion modes in the 1,1-dimethylhydrazine ion and in the transition states were treated separately according to the East and Radom[3] procedure for the computation of third-law entropies. In this procedure, the two methyl torsion modes, which are the two lowest vibrational frequencies (111 and 139 cm^{-1}) in the 1,1-dimethylhydrazine ion, were treated first with the harmonic oscillator model and second as free rotors. For the free rotor model, the internal moment of inertia was estimated to be between 3.0 and 3.1 amu Å^2. These values were taken from Table 7 in the East and Radom[3] paper, which lists

Fragmentation of 1,1-Dimethylhydrazine Ions

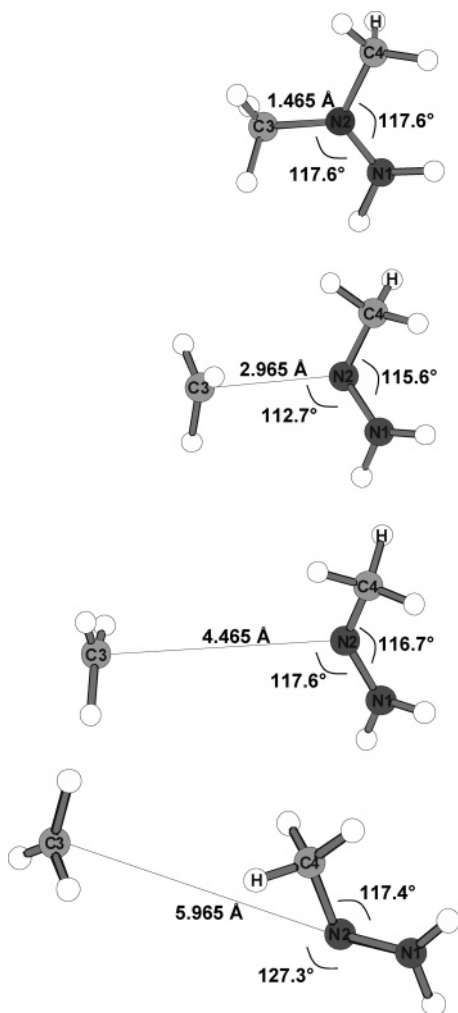*J. Phys. Chem. A, Vol. 111, No. 25, 2007* **5393**

Figure 4. Structures of the 1,1-dimethylhydrazine ion and its dissociating complexes for the loss of a methyl group calculated at the B3-LYP/6-31+G(d) level of theory.
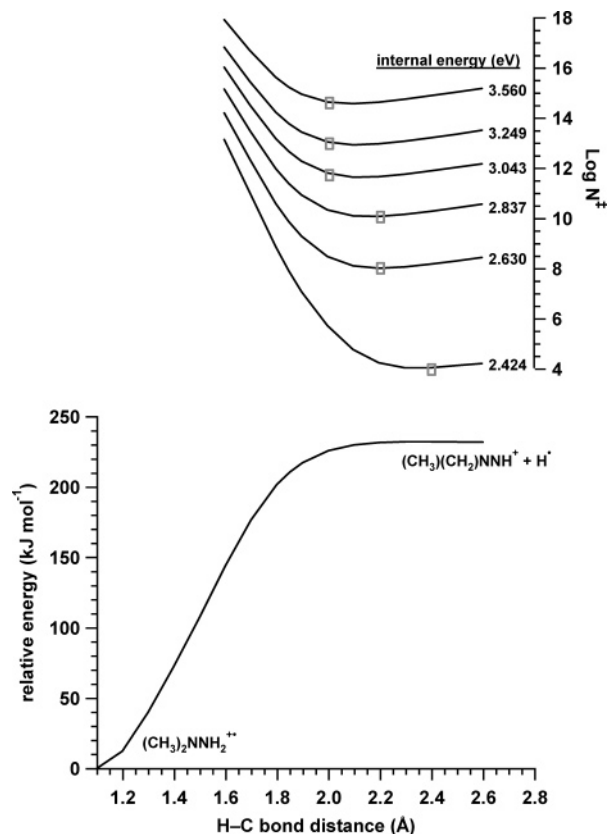

Figure 5. Potential energy curve for the loss of a hydrogen atom from the 1,1-dimethylhydrazine ion and the sum-of-states as a function of the H−C bond distance calculated at the B3-LYP/6-31+G(d) level of theory. The squares correspond to the minimum in $N^{\ddagger}$ and thus the transition states for the H−C bond cleavage.

the calculated internal moments of inertia of various single and multiple rotors. In the case of the hydrogen loss channel, the hydrogen atom comes from one of the two methyl groups. Therefore, the system was treated as having only one free rotor which corresponds to the intact methyl group.

Results and Discussion

Reaction Mechanisms. The MIKE mass spectrum of ionized 1,1-dimethylhydrazine shows peaks at m/z 45 and m/z 59. These two peaks correspond to the loss of a methyl group to form the ion m/z 45 with the empirical formula $CH_5N_2^+$ and to the loss of a hydrogen atom to form the ion m/z 59 with the empirical formula $C_2H_7N_2^+$. The MIKE and CID mass spectra of the fragment ion m/z 45 are consistent with the methylhydrazyl cation structure $CH_3NNH_2^+$ reported by Burgers et al.[14] in their study of the CH_5N_2 hydrazyl radicals and cations. We also generated $(CH_3)_2NND_2^{+\bullet}$ (see Experimental Procedures) which showed only H loss in both MIKE and CID mass spectra, thereby confirming that m/z 59 is $(CH_3)(CH_2)NNH_2^+$.

Potential Energy Curves. The relative energies of the 1,1-dimethylhydrazine ion and its fragment ions and neutrals have been calculated at the B3-LYP/6-31+G(d) level of theory and with a modified G3 protocol (Table 2). At the B3-LYP/6-31+G-(d) level of theory, the two sets of dissociation products [CH_3-NNH_2^+ + $CH_3^{\bullet}$] and [$(CH_3)(CH_2)NNH_2^+$ + $H^{\bullet}$] have similar energies. However, their G3 energies place the hydrogen loss

channel lower by 19 kJ mol^{-1}. The relative energy of the second possible structure of the ion m/z 59 ($(CH_3)_2NNH^+$) was also calculated. However, this dissociation is not energetically favorable because it is 36 kJ mol^{-1} higher in energy than hydrogen loss from the methyl group at the G3 level of theory. The fact that no D loss is observed in the CID mass spectrum of the labeled ion confirms that H loss from N does not compete significantly with H loss from C, even for ions with relatively high internal energy.

The potential energy curve for the loss of a methyl group is shown in Figure 2 together with the sum-of-states calculated as a function of the N−C bond distance. Figure 3 shows the five lowest vibrational frequencies and the $\Delta S^{\ddagger}$ as a function of N−C bond distance. Six vibrational modes disappear when the 1,1-dimethylhydrazine ion dissociates into the fragment ion $CH_3NNH_2^+$ + $CH_3^{\bullet}$. One mode corresponds to one N−C stretch, the reaction coordinate, and the five other modes correspond to deformation, torsion, and scissoring involving a methyl group. An inflection point and two distinct local maxima are noticeable in the sum-of-states plot (Figure 2, top graph), one at R_{N-C} = 2.16 Å, one at R_{N-C} = 3.56 Å, and one around R_{N-C} = 4.86−4.96 Å. The first feature at 2.16 Å is consistent with a sudden change in the H−CH$_2$ wagging vibrational frequency of the dissociating complex between R_{N-C} = 2.16−2.36 Å (Figure 3). The changes in the vibrational frequencies affect the value of the $\Delta S^{\ddagger}$. At that N−C bond distance, a local maximum is observed in the $\Delta S^{\ddagger}$ (Figure 3). At R_{N-C} = 3.56 Å there is a local maximum on the plot of N even though there is no obvious change in the vibrational frequencies. As the N−CH$_3$ bond is stretched, the two smaller rotational constants slowly decrease from their initial values in the equilibrium
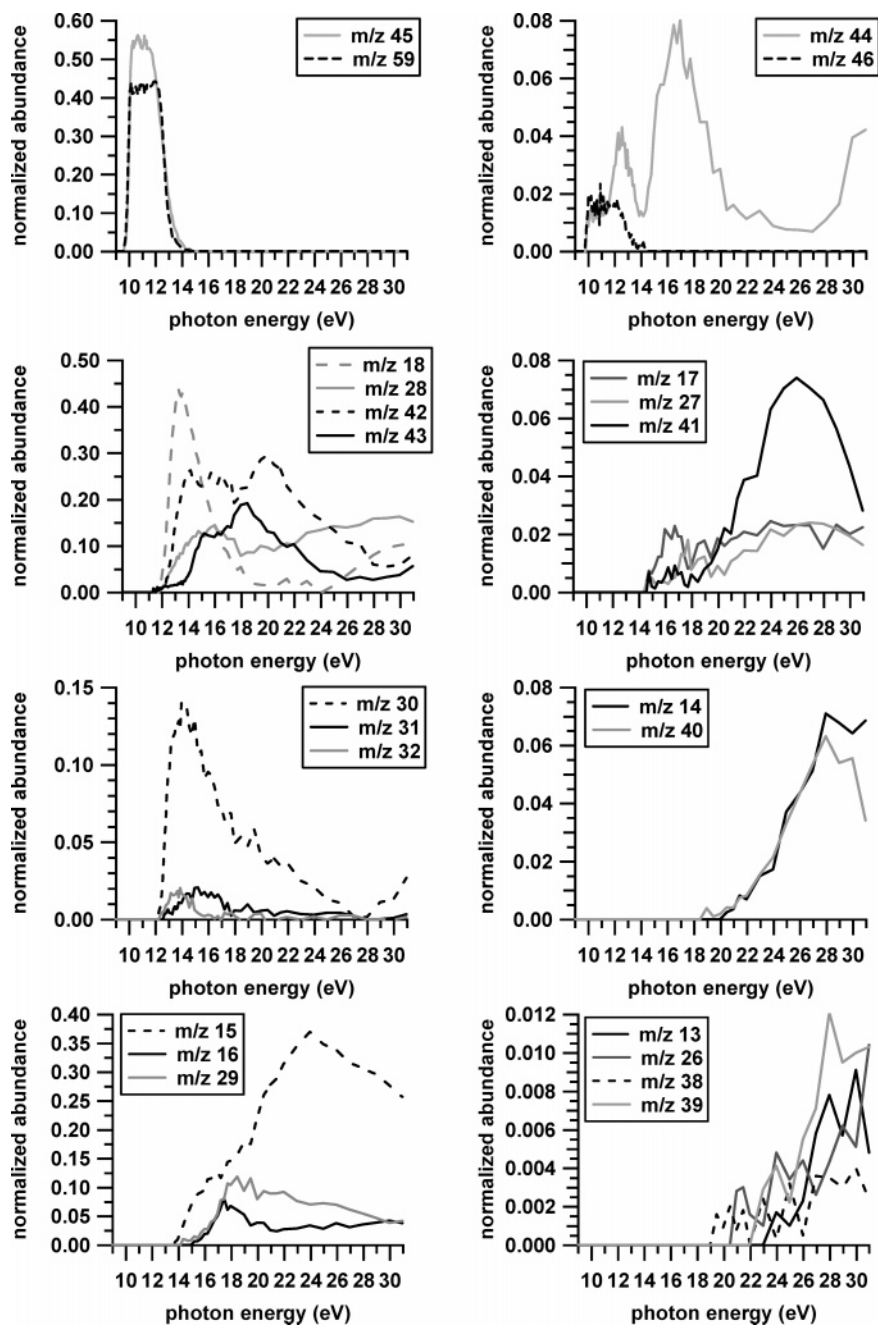
Figure 6. Relative abundances of all fragment ions of 1,1-dimethylhydrazine in the photon energy range 9−31 eV.

geometry. The third local maximum in the sum-of-states, at $R_{N-C} = 4.86-4.96$ Å, corresponds to a slight dip in energy for this complex. This dip is due to the crossing of the potential energy curve for the loss of methyl with that for the dissociation of a second high-energy species having the geometry shown in the last panel of Figure 4. Starting at higher values of R_{N-C} and optimizing the geometry at successively shorter bond lengths results in a discontinuity at $R_{N-C} = 4.86$ Å, but it was impossible to optimize the lower energy structure below $R_{N-C} = 4.66$ Å. The methyl group is now situated above the $CH_3NNH_2^+$ fragment ion (Figure 4). Fortunately, this point is at a higher R_{N-C} value than the variational transition states.

Figure 5 shows the potential energy curve and the sum-of-states for the loss of a hydrogen atom from one of the two methyl groups. Three vibrational modes, one corresponding to the reaction coordinate (H−C stretch) and the two others to H−C scissoring or wag are converted to translational degrees

of freedom of the hydrogen atom in this dissociation. There are no local maxima in the plot of the sum-of-states for hydrogen loss.

The transition states for each channel were identified by finding the minima in the sum-of-states as a function of internal energy and are listed in Tables 3 and S2. Table 3 lists the transition states for the B3-LYP/6-31+G(d) potential energy curves and the corrected curves (see Variational Fits), and Table S2 in the Supporting Information lists the vibrational frequencies and the rotational constants for the 1,1-dimethylhydrazine ion, its dissociation products, and the various transition states. For the methyl loss reaction, nine transition states are listed in Table S2, of which six or seven are active for a particular fit of E_0 (see Table 3). Likewise, three transition states are listed for the hydrogen loss reaction, of which two or three are active for a particular fit of E_0. For the methyl loss channel at the B3-LYP/6-31+G(d) level of theory, seven transition states were found
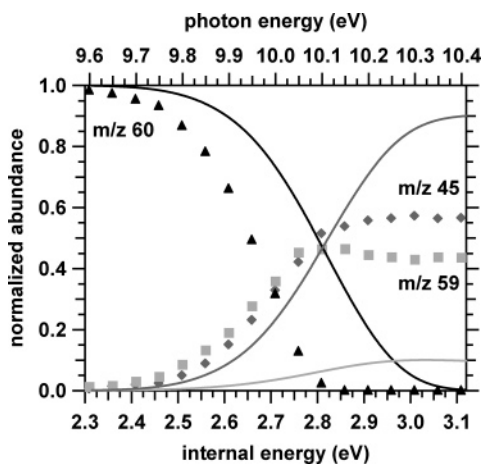
Fragmentation of 1,1-Dimethylhydrazine Ions

J. Phys. Chem. A, Vol. 111, No. 25, 2007 **5395**

Figure 7. Comparison between the experimental breakdown curve and the theoretical fit at a parent ion residence time of 1.116 μs using the variational transition states at the B3-LYP/6-31+G(d) energies corrected to the G3 fragment products energies. The parent ion m/z 60 is represented by ▲, the fragment ion m/z 45 is represented by ◆, and the fragment ion m/z 59 is represented by ■. The theoretical fits are represented by the solid lines (black for parent ion m/z 60, dark gray for fragment ion m/z 45, and light gray for ion m/z 59).

in the internal energy range of 2.32−3.56 eV. For the hydrogen atom loss channel, three transition states were found in the same energy range. As expected from VTST, the transition states move to shorter N−C or H−C bond distance as the internal energy of the dissociating complex increases. There is a large change in the $\Delta S^{\ddagger}$ for the methyl loss channel over the studied internal energy range. $\Delta S^{\ddagger}$ varies from 65 J K^{-1} mol^{-1} at E_{int} = 2.32 eV to 29 J K^{-1} mol^{-1} at E_{int} = 3.56 eV. In the case of the hydrogen loss channel, the $\Delta S^{\ddagger}$ values are small (8 to 0.9 J K^{-1} mol^{-1}) and do not vary as much as those for the methyl loss channel.

Breakdown Curves. The 1,1-dimethylhydrazine ion breakdown curve has been recorded between $h\nu$ = 8.25 and $h\nu$ = 31.00 eV, and a total of 23 fragment ions were observed. Employing the adiabatic ionization energy of 7.29 ± 0.04 eV[15] yields an internal energy range of 0.96−23.71 eV. Our previous TPES value of 7.78 ± 0.16 eV[16] was demonstrated to be too high due to the large geometry change upon ionization. Figure 6 shows the relative abundances for all the fragment ions as a function of photon energy. As mentioned previously, the first two dissociation channels are the loss of a methyl group and the loss of a hydrogen atom to form the fragment ions m/z 45 ($CH_3NNH_2^+$) and m/z 59 ($(CH_3)(CH_2)NNH_2^+$), respectively.

TABLE 4: AEs of Fragment Ions of the 1,1-Dimethylhydrazine Ion

| m/z	ion fragment	AE (eV)	ionization technique	reference
59	$(CH_3)(CH_2)NNH_2^+$	9.65 ± 0.05	TPEPICO	present work
		8.7 ± 0.2	photoionization	Akopyan and Vilesov[21]
		10.08 ± 0.1	electron ionization	Foner and Hudson[19]
		10.2 ± 0.2	electron ionization	Dibeler et al.[20]
		10.0 ± 0.3	electron ionization	Foner and Hudson[18]
58	$C_2H_6N_2^+$	9.5 ± 0.1	photoionization	Akopyan and Vilesov[21]
46	$CH_6N_2^+$ or $C_2H_8N^+$	9.80 ± 0.05	TPEPICO	present work
45	$CH_3NNH_2^+$	9.65 ± 0.05	TPEPICO	present work
		8.4 ± 0.1	photoionization	Akopyan and Vilesov[21]
		8.60	electron ionization	Burgers et al.[14]
		9.7 ± 0.2	electron ionization	Dibeler et al.[20]
	$(CH_3)_2NH^+$	11.2 ± 0.2	photoionization	Akopyan and Vilesov[21]
44	$C_2H_6N^+$	9.85 ± 0.05	TPEPICO	present work
		9.0 ± 0.2	photoionization	Akopyan and Vilesov[21]
		11.2 ± 0.2	photoionization	Akopyan and Vilesov[21]
		10.45 ± 0.05	electron ionization	Fisher and Henderson[22]
		10.7 ± 0.1	electron ionization	Gowenlock et al.[23]
		10.9 ± 0.2	electron ionization	Dibeler et al.[20]
43	$C_2H_5N^+$	11.35 ± 0.05	TPEPICO	present work
		8.8 ± 0.1	photoionization	Akopyan and Vilesov[21]
		10.9 ± 0.2	photoionization	Akopyan and Vilesov[21]
		12.5 ± 0.2	electron ionization	Dibeler et al.[20]
		13.5 ± 0.2	electron ionization	Dibeler et al.[20]
42	$C_2H_4N^+$	11.65 ± 0.10	TPEPICO	present work
		12.8 ± 0.2	electron ionization	Dibeler et al.[20]
41	$C_2H_3N^+$	14.75 ± 0.20	TPEPICO	present work
40	$C_2H_2N^+$	18.95 ± 0.50	TPEPICO	present work
39	C_2HN^+	22.95 ± 1.00	TPEPICO	present work
38	C_2N^+	19.45 ± 0.50	TPEPICO	present work
32	$N_2H_4^+$	12.35 ± 0.10	TPEPICO	present work
31	$N_2H_3^+$	12.65 ± 0.10	TPEPICO	present work
30	$N_2H_2^+$	12.25 ± 0.10	TPEPICO	present work
		8.6 ± 0.1	photoionization	Akopyan and Vilesov[21]
		12.9 ± 0.1	electron ionization	Dibeler et al.[20]
29	N_2H^+ or $CH_2{=}NH^+$	14.35 ± 0.20	TPEPICO	present work
		14.2 ± 0.5	electron ionization	Dibeler et al.[20]
28	N_2^+	11.85 ± 0.10	TPEPICO	present work
		13.2 ± 0.1	electron ionization	Dibeler et al.[20]
27	HCN^+	14.55 ± 0.20	TPEPICO	present work
26	CN^+	20.95 ± 0.50	TPEPICO	present work
18	NH_4^+	11.75 ± 0.10	TPEPICO	present work
17	NH_3^+	14.55 ± 0.20	TPEPICO	present work
16	NH_2^+	15.20 ± 0.25	TPEPICO	present work
		13.3 ± 0.1	electron ionization	Gowenlock et al.[23]
15	CH_3^+	13.75 ± 0.10	TPEPICO	present work
		14.5 ± 0.3	electron ionization	Dibeler et al.[20]
14	CH_2^+	20.45 ± 0.50	TPEPICO	present work
13	CH^+	23.95 ± 1.00	TPEPICO	present work
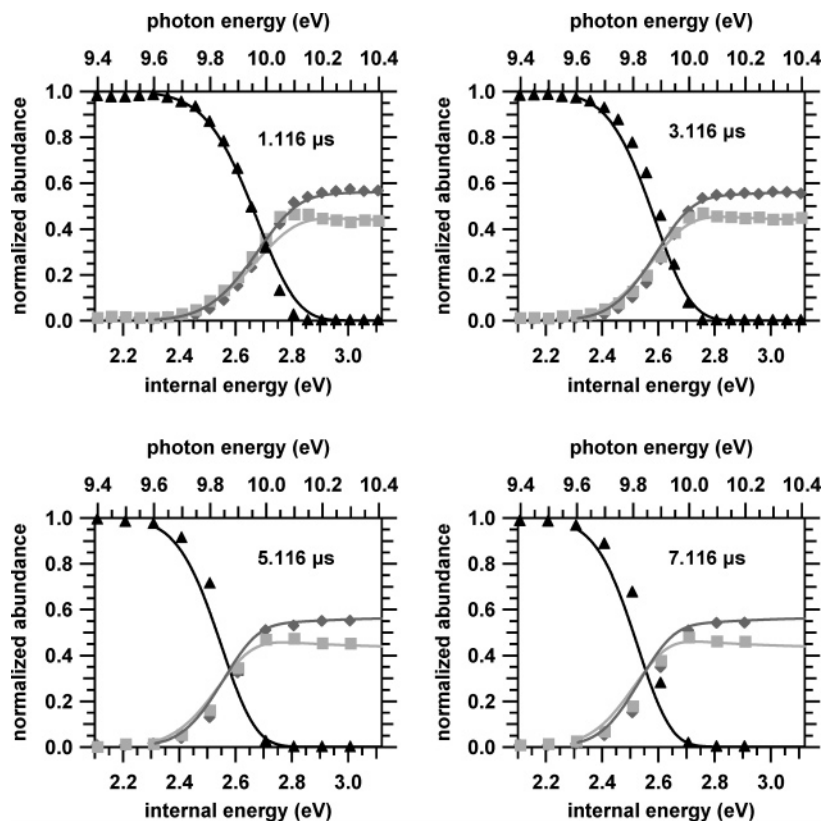
Figure 8. Comparison between the experimental breakdown curves and the theoretical fit (fit 2) using seven variational transition states for the methyl loss and two transition states for hydrogen loss. The energy differences between the 1,1-dimethylhydrazine ion and the potential energy curve plateau are $\Delta E(45) = 2.330$ eV and $\Delta E(59) = 2.155$ eV. The parent ion m/z 60 is represented by (▲), the fragment ion m/z 45 is represented by ◆, and the fragment ion m/z 59 is represented by ■. The theoretical fits are represented by the solid lines (black for parent ion m/z 60, dark gray for fragment ion m/z 45, and light gray for ion m/z 59).
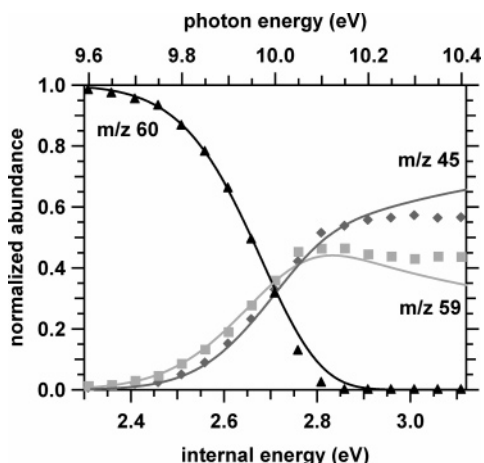
Figure 9. Comparison between the experimental breakdown curve and the theoretical fit at a parent ion residence time of 1.116 μs using one transition state for each dissociation channel ($E_0(45) = 2.314$ eV and $E_0(59) = 2.152$ eV). The parent ion m/z 60 is represented by ▲, the fragment ion m/z 45 is represented by ◆, and the fragment ion m/z 59 is represented by ■. The theoretical fits are represented by the solid lines (black for parent ion m/z 60, dark gray for fragment ion m/z 45, and light gray for ion m/z 59).

The parent ion m/z 60 is not observed at photon energies greater than 10.15 eV. Over the next $\sim$ 1.6 eV, the only fragment ions detected are m/z 45 and m/z 59, and these occur with a constant ratio. Ions m/z 44 and 46 have onsets at $h\nu$ = 9.85 and 9.80 eV (E_{int} = 2.56 and 2.51 eV), respectively, but their abundances are low (less than 2%), while the abundances of ions m/z 45 and 59 are 55 and 45%, respectively. One interesting feature in the first crossover region of the breakdown curve (Figure 7) is

that ion m/z 59 is more intense than ion m/z 45 up to $h\nu$ = 10.05 eV (E_{int} = 2.76 eV) where the two product curves cross. At a photon energy of $h\nu$ = 11.75 eV (E_{int} = 4.46 eV), higher energy dissociation products start to appear. The most intense ions are m/z 18 (NH_4^+) and m/z 42 ($C_2H_4N^+$). MIKE and CID experiments indicate that the NH_4^+ ion is most probably formed from $CH_3NNH_2^+$ while the m/z 42 ion is a fragment produced from the decomposition of m/z 59. As the photon energy increases further, two other ions, m/z 30 ($N_2H_2^+$) from m/z 59 and m/z 28 (N_2^+) from m/z 45, slowly form. Tentative structures or empirical formulas have been assigned to each fragment ion and can be found in Table 4. This table also contains the previous experimental AEs as well as an indication of the ionization technique used to generate the fragment ions.

Variational Fits. The fit of the experimental breakdown curves using the above calculated VTST $k(E_{int})$ for each channel at the B3-LYP/6-31+G(d) level of theory was poor. There are two reasons why the VTST treatment may not be satisfactory. First, the B3-LYP/6-31+G(d) values for E_0 are certainly in error, and second the location of the transition states (and hence $\Delta S^\ddagger$) may be poorly described with the VTST approach employed herein. We corrected the B3-LYP/6-31+G(d) potential energy curves so the plateau corresponded to the G3 product energies to correct for an inaccurate E_0. The fit to the experimental data was greatly improved but was still in need of refinement (Figure 7). The five lowest vibrational frequencies of the transition states for the hydrogen loss channel were then scaled to change $\Delta S^\ddagger$ for this channel from 0.9–7.9 J K^{-1} mol^{-1} to 16–26 J K^{-1} mol^{-1}. In addition the potential energy curves for the two channels were adjusted up or down to obtain a good fit to the data (Figure 8). The results for all of these attempts are

Fragmentation of 1,1-Dimethylhydrazine Ions

J. Phys. Chem. A, Vol. 111, No. 25, 2007 **5397**

TABLE 5: Enthalpies of Formation of $(CH_3)_2NNH_2^{+\bullet}$, $(CH_3)(CH_2)NNH_2^+$, $CH_3NNH_2^+$ and Fragment Neutrals

m/z	ion or neutral	$\Delta_f H$ (kJ mol^{-1})	method	reference
60	$(CH_3)_2NNH_2^{+\bullet}$	831	G3 calculations (0 K)	present work
		804	G3 calculations (298 K)	Boulanger et al.[16]
59	$(CH_3)(CH_2)NNH_2^+$	822 ± 7	VTST fit (0 K)	present work
		825	G3 calculations (0 K)	present work
		801	G3 calculations (298 K)	present work
		845	electron ionization	Dibeler et al.[20]
		820	photoionization	Akopyan and Vilesov[21]
45	$CH_3NNH_2^+$	906 ± 6	VTST fit (0 K)	present work
		911	G3 calculations (0 K)	present work
		893	G3 calculations (298 K)	present work
		883	electron ionization	Dibeler et al.[20]
		787	photoionization	Akopyan and Vilesov[21]
		767.8	electron ionization	Burgers et al.[14]
	$CH_3^\bullet$	149	G3 calculations (0 K)	present work
		146	G3 calculations (298 K)	present work
	$H^\bullet$	216	G3 calculations (0 K)	present work
		212	G3 calculations (298 K)	present work

summarized in Table 3. In the end, only small changes were needed to the energy of the potential energy curves relative to the G3 results. It is important to note that the value of the adiabatic ionization energy has an effect on the fits of the breakdown curves. When using the calculated G3 IE_a value of 7.36 eV[16] instead of the reported value of 7.29 ± 0.04 eV by Meot-Ner et al.,[15] the values of E_0 for the methyl loss channel did not need to be adjusted to fit the experimental breakdown curves (see Table 3 for E_0 values of methyl loss channel); only the E_0 values for the hydrogen loss channel had to be changed ($E_0(R_{H-C} = 2.20$ Å$) = 2.122$ eV and $E_0(R_{H-C} = 2.10$ Å$) = 2.105$ eV). These differences in E_0 are taken into account in the uncertainties of the resulting $\Delta_f H$ values (see Enthalpies of Formation).

We also tried fitting the experimental breakdown curves without VTST, employing only one transition state for each dissociation channel. In this fit, the transition state used for the methyl loss was at $R_{N-C} = 3.46$ Å and for hydrogen atom loss, and the transition state used was at $R_{H-C} = 2.20$ Å. The E_0 and vibrational frequencies of both channels were changed to find the best agreement with the experimental data. However, it was not possible to find one set of energies and vibrational frequencies that would fit all the experimental data simultaneously. Figure 9 shows the best theoretical fit to the 1.116 μs residence time breakdown curve using a single transition state for each dissociation channel. Satisfactory fits to the parent and the total product curves could be obtained but not for the individual product curves. Each product curve (m/z 45 and m/z 59) could be fitted up to $E_{int} = 2.91$ eV but the plateau above that energy could not be reproduced. Having only one transition state for the methyl loss could not take into account the large change in the $\Delta S^\ddagger$ with increasing internal energy observed in the variational analysis.

Appearance Energies. In the present work, twenty-three fragment ions were observed in the dissociation of 1,1-dimethylhydrazine as the photon energy was increased from the ionization threshold to $h\nu = 31$ eV. The AEs of some of these fragments have been reported previously using electron ionization or photoionization techniques, and Table 4 provides a summary of the results. It should be kept in mind that experimentally determined AEs may be subject to kinetic and competitive shifts and/or reverse energy barriers[17] and therefore should be regarded as upper limits to the thermochemical thresholds.

The AEs of the fragment ion m/z 59 reported by Foner and Hudson[18,19] and by Dibeler et al.[20] are ∼0.5 eV higher than our

value. In these studies,[18−20] the $(CH_3)_2NNH^+$ structure was proposed for this ion. However, the results of our G3 calculations show that this ion is actually 36 kJ mol^{-1} higher in energy than $(CH_3)(CH_2)NNH_2^+$.

The various AEs for the fragment ion m/z 45 (Table 4) differ considerably from one another. The value reported by Dibeler et al.[20] (9.7 ± 0.2 eV) is in accord with our AE of 9.65 ± 0.05 eV. However, Akopyan and Vilesov[21] and Burgers et al.[14] give values which are more than 1 eV lower. Akopyan and Vilesov[21] have also reported an AE of 11.2 ± 0.2 eV for another possible structure of m/z 45, $(CH_3)_2NH^+$. All previous AEs for the fragment ion m/z 44 lie 0.6−1.0 eV higher than our value of 9.85 ± 0.05 eV, except that measured by Akopyan and Vilesov,[21] which is 0.85 eV lower. Fisher and Henderson[22] have proposed a structure of $(CH_3)_2N^+$ for the m/z 44 ion, although $CH_3NHCH_2^+$ may be more favorable. Previous AEs for the fragment ion m/z 43 differ significantly from our experimental result of 11.35 ± 0.05 eV. Dibeler et al.[20] reported two AEs (12.5 ± 0.2 and 13.5 ± 0.2 eV) for this ion, as did Akopyan and Vilesov[21] (8.8 ± 0.1 and 10.9 ± 0.2 eV). For m/z 42, Dibeler et al.[20] give an AE of 12.8 ± 0.2 eV, compared to our value of 11.65 ± 0.05 eV, and suggest that the fragment ion is $(CH_2)_2N^+$. Our AEs for the fragment ions m/z 30 ($N_2H_2^+$) and m/z 29 (N_2H^+) are in good agreement with those measured by Dibeler et al.,[20] but the AE reported by Akopyan and Vilesov[21] for the m/z 30 fragment ion differs considerably.

Our AE for the N_2^+ fragment is lower by ∼1.4 eV than that given by Dibeler et al.[20] Fragment ion m/z 16, corresponding to NH_2^+, has an AE of 15.20 ± 0.25 eV, which is higher than that reported by Gowenlock et al.,[23] and finally, the methyl cation, CH_3^+, has an AE of 13.75 ± 0.10 eV, which is close to that determined by Dibeler et al.[20]

No AEs are available for the other fragment ions observed in the present work. Akopyan and Vilesov[21] report an AE of 9.5 ± 0.1 eV for the fragment ion m/z 58, but we did not observed this ion, pointing to possible contamination of their sample. The m/z 58 ion is observed in our MIKE and CID mass spectra of $(CH_3)(CH_2)NNH_2^+$, m/z 59.

Enthalpies of Formation. The $\Delta_f H$ values for the fragment ions m/z 45 and m/z 59 have also been determined from the variational fits of the breakdown curves and from the G3 calculations. These results are listed in Table 5 together with previous data. The enthalpies of formation have been determined from the following equations:[9]

$$AB + e^- \rightarrow AB^{+\bullet} + 2e^- \tag{7}$$

$$AB^{+\bullet} \rightarrow A^+ + B^\bullet \tag{8}$$
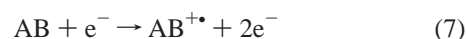
$$\Delta_f H_0(A^+) = E_0(A{-}B^{+\bullet}) + \Delta_f H_0(AB^{+\bullet}) - \Delta_f H_0(B^\bullet) \tag{9}$$

The $\Delta_f H_0$ of the parent ion $AB^{+\bullet}$ and neutral fragment $B^\bullet$ were taken from our G3 calculations (Table 5). To calculate $\Delta_f H_0$ from the VTST results, the E_0 for the transition state found at the lowest internal energy studied was used. This value will technically always be lower than the true thermochemical threshold because the transition states do not sit at products. The $\Delta_f H_0$ values are listed in Table 5. The uncertainty in the enthalpy of formation takes into account the uncertainties in the IE_a value, the E_0 values, and the photon energy.

The derived $\Delta_f H_0$ of $(CH_3)(CH_2)NNH_2^+$ compares well with the calculated G3 value, 822 ± 7 versus 825 kJ mol^{-1}, respectively. Both of these values are lower than the 845 kJ mol^{-1} reported by Dibeler et al.,[20] based upon electron ionization studies of 1,1-dimethylhydrazine and trimethylhydrazine. Akopyan and Vilesov[21] obtained a value of 820 kJ mol^{-1}. The VTST/experimentally derived $\Delta_f H_0$ value for $CH_3NNH_2^+$ is 906 $\pm$ 6 kJ mol^{-1} compared to 911 kJ mol^{-1} from G3 calculations. Hence, the results obtained through these two methods are in good agreement. Both of these values are higher than the 883 kJ mol^{-1} reported by Dibeler et al.[20] The $\Delta_f H$ value of Burgers et al.,[14] 768 kJ mol^{-1}, and that of Akopyan and Vilesov,[21] 787 kJ mol^{-1}, are more than 100 kJ mol^{-1} lower than our calculated values as their AEs were measured to be more than 1 eV lower than the present results. We can find no obvious explanation for this discrepancy and believe the previous results are in error.

Summary

The 1,1-dimethylhydrazine ion has two low-energy dissociation channels: the loss of a methyl radical to form the methylhydrazyl cation, $CH_3NNH_2^+$, and the loss of a hydrogen atom to form $(CH_3)(CH_2)NNH_2^+$. VTST was used to locate the transition states for the two channels. At the B3-LYP/6-31+G-(d) level of theory, for methyl loss, seven transition states were found in the internal energy range of 2.32–3.56 eV while three were found for hydrogen loss, which reflect a large change in $\Delta S^\ddagger$ for each channel over this internal energy range. The VTST results were adjusted very slightly to obtain a theoretical fit of the TPEPICO breakdown diagrams recorded at four different parent ion reaction times. It was not possible to reproduce the experimental change in product ion abundance with internal energy employing a single transition state for each channel. Enthalpies of formation for fragment ions m/z 45, $CH_3NNH_2^+$, and m/z 59, $(CH_3)(CH_2)NNH_2^+$, as determined from the VTST fits to the TPEPICO data, were found to be in excellent agreement with those from G3 calculations. In the photon energy range (threshold to 31 eV) used to study the dissociation of the 1,1-dimethylhydrazine ion, a total of 23 fragment ions were observed, and their AEs have been reported.

Supporting Information Available: Tables of rate constants, vibrational frequencies, and rotational constants and figure of potential energy curves. This material is available free of charge via the Internet at http://pubs.acs.org.

References and Notes

(1) Baer, T.; Hase, W. L. *Unimolecular Reactions Dynamics - Theory and Experiments*; Oxford University Press: New York, 1996.

(2) Baer, T.; Mayer, P. M. *J. Am. Soc. Mass Spectrom.* **1997**, *8*, 103.

(3) East, A. L. L.; Radom, L. *J. Chem. Phys.* **1997**, *106*, 6655.

(4) Lifshitz, C.; Louage, F.; Aviyente, V. *J. Phys. Chem.* **1991**, *95*, 9298.

(5) Holland, D. M. P.; Shaw, D. A.; Sumner, I.; Hayes, M. A.; Mackie, R. A.; Wannberg, B.; Shpinkova, L. G.; Rennie, E. E.; Cooper, L.; Johnson, C. A. F.; Parker, J. E. *Nucl. Instr. Methods Phys. Res. B* **2001**, *179*, 436.

(6) Holland, D. M. P.; West, J. B.; Macdowell, A. A.; Munro, I. H.; Beckett, A. G. *Nucl. Instr. Methods Phys. Res. B* **1989**, *44*, 233.

(7) Rennie, E. E.; Boulanger, A.-M.; Mayer, P. M.; Holland, D. M. P.; Shaw, D. A.; Cooper, L.; Shpinkova, L. G. *J. Phys. Chem. A* **2006**, *110*, 8663.

(8) Rennie, E. E.; Cooper, L.; Johnson, C. A. F.; Parker, J. E.; Mackie, R. A.; Shpinkova, L. G.; Holland, D. M. P.; Shaw, D. A.; Hayes, M. A. *Chem. Phys.* **2001**, *263*, 149.

(9) Holmes, J. L.; Mayer, P. M. *J. Phys. Chem.* **1995**, *99*, 1366.

(10) Frisch, M. J.; Trucks, G. W.; Schlegel, H. B.; Scuseria, G. E.; Robb, M. A.; Cheeseman, J. R.; Zakrzewski, V. G.; Montgomery, J. A., Jr.; Stratmann, R. E.; Burant, J. C.; Dapprich, S.; Millam, J. M.; Daniels, A. D.; Kudin, K. N.; Strain, M. C.; Farkas, O.; Tomasi, J.; Barone, V.; Cossi, M.; Cammi, R.; Mennucci, B.; Pomelli, C.; Adamo, C.; Clifford, S.; Ochterski, J.; Petersson, G. A.; Ayala, P. Y.; Cui, Q.; Morokuma, K.; Malick, D. K.; Rabuck, A. D.; Raghavachari, K.; Foresman, J. B.; Cioslowski, J.; Ortiz, J. V.; Stefanov, B. B.; Liu, G.; Liashenko, A.; Piskorz, P.; Komaromi, I.; Gomperts, R.; Martin, R. L.; Fox, D. J.; Keith, T.; Al-Laham, M. A.; Peng, C. Y.; Nanayakkara, A.; Gonzalez, C.; Challacombe, M.; Gill, P. M. W.; Johnson, B. G.; Chen, W.; Wong, M. W.; Andres, J. L.; Head-Gordon, M.; Replogle, E. S.; Pople, J. A. *Gaussian 98*, revision A.6; Gaussian, Inc.: Pittsburgh, PA, 1998.

(11) Curtiss, L. A.; Raghavachari, K.; Redfern, P. C.; Rassolov, V.; Pople, J. A. *J. Chem. Phys.* **1998**, *109*, 7764.

(12) Nicolaides, A.; Rauk, A.; Glukhovtsev, M. N.; Radom, L. *J. Phys. Chem.* **1996**, *100*, 17460.

(13) Atkins, P. W. *Physical Chemistry*, 6th ed.; W. H. Freeman and Company: New York, 1998.

(14) Burgers, P. C.; Drewello, T.; Schwarz, H.; Terlouw, J. K. *Int. J. Mass Spectrom. Ion Processes* **1989**, *95*, 157.

(15) Meot-Ner, M.; Nelsen, S. F.; Willi, M. R.; Frigo, T. B. *J. Am. Chem. Soc.* **1984**, *106*, 7384.

(16) Boulanger, A.-M.; Rennie, E. E.; Holland, D. M. P.; Shaw, D. A.; Mayer, P. M. *J. Phys. Chem. A* **2006**, *110*, 8563.

(17) Cooks, R. G.; Beynon, J. H.; Caprioli, R. M.; Lester, G. R. *Metastable Ions*; Elsevier: Amsterdam, 1973.

(18) Foner, S. N.; Hudson, R. L. *Adv. Chem. Ser.* **1962**, *36*, 34.

(19) Foner, S. N.; Hudson, R. L. *J. Chem. Phys.* **1970**, *53*, 4377.

(20) Dibeler, V. H.; Franklin, J. L.; Reese, R. M. *J. Am. Chem. Soc.* **1959**, *81*, 68.

(21) Akopyan, M. E.; Vilesov, F. I. *Kinet. Katal.* **1963**, *4*, 39.

(22) Fisher, I. P.; Henderson, E. *J. Chem. Soc., Faraday Trans.* **1967**, *63*, 1342.

(23) Gowenlock, B. G.; Jones, P. P.; Majer, J. R. *Trans. Faraday Soc.* **1961**, *57*, 23.